Morphological Investigation of Hybrid Langmuir−Blodgett Films of Arachidic Acid with a Hydrotalcite/Dendrimer Nanocomposite

Alexsandro Santos Costa[†] and Toyoko Imae*[,†,‡]

Graduate School of Science and Research Center for Materials Science, Nagoya University, Chikusa, Nagoya 464-8602, Japan

Received April 10, 2004. In Final Form: June 27, 2004

A hydrotalcite clay/dendrimer nanocomposite prepared by the ionic exchange process was adsorbed from suspension of the nanocomposite on a Langmuir monolayer of arachidic acid at the air/water interface, followed by compressing and transferring onto an arachidic acid monolayer Langmuir−Blodgett (LB) film on mica. For comparison, the hydrotalcite-adsorbed hybrid film was also prepared. The morphology of hydrotalcite and the nanocomposite studied by transmission electron microscopy indicated the layered structures with respectively 1.2 ± 0.3 and 3.2 ± 0.5 nm repeating distances. The hybrid Langmuir films displayed the occupied surface area of 0.24 nm^2 for both hydrotalcite and the nanocomposite. The formation of hybrid Langmuir films was confirmed by Brewster angle microscopy. Atomic force microscopic images of hybrid LB films revealed the formation of plateau domains with the height difference of 6 nm for hydrotalcite and 12 nm for the nanocomposite and the presence of dendrimers adsorbed on the clay surface of the nanocomposite.

Downloaded by NATL TAIWAN UNIV SCIENCE & TECHLGY at 10:37:36:622 on June 25, 2019
from https://pubs.acs.org/doi/10.1021/la049088a.

Introduction

The construction of nanostructured inorganic/organic materials provides a practicle chemical approach to the preparation of advanced materials for application to optics and electronics. The self-assembly consisting of positively and negatively charged species has been developed for many nanocomposites[1−3] including clay/polyelectrolytes.[4−7] On the other hand, the organization of nanostructured materials into thin films is also required in many applications. Among various film preparation techniques, the Langmuir−Blodgett (LB) method is suitable for resulting in highly ordered films of nanocomposites. Design of controlled clay multilayers using the LB technique has been reported.[8] Moreover, the production of a clay monolayer at the air/water interface has also been accomplished.[9] Electrostatic or hydrogen-bonding interaction at the interface functions in the preparation of these films.

Hydrotalcite is a layered clay material possessing anion-exchange capacity as a result of partial substitution of bivalent cations by trivalent ones in the clay framework, developing a positive net charge in the structure. Molecules such as water, carbonate, nitrate, and chloride anions are located in the clay interlayer to balance the charges developed by the partial substitution of cations. However, most of them are easily exchanged depending on the competitive clay charge affinity to the foremost-located anions and the extrinsic ones.[10−16] Intercalation of various molecules in the clay structure through anionic exchange results in materials with budding functionality to be used from catalysts to ceramic-based nanocomposites.[17−22]

We have focused on the preparation of nanocomposites through the diffusion of dendrimer and dendrimer-protected silver nanoparticles into the layered structure of hydrotalcite by anion exchange.[23,24] The expansion of the clay interlayer, revealed by X-ray diffraction and small-angle X-ray scattering, indicates the intercalation of dendrimers and nanoparticles into hydrotalcite. In another study by X-ray reflectometry, the structural details in films of clay and clay/dendrimer nanocomposites were investigated.[25] Although these studies clarified the quan-

* To whom correspondence should be addressed. Fax: +81-52-789-5912. E-mail: imae@nano.chem.nagoya-u.ac.jp. Phone: +81-52-789-5911.

[†] Graduate School of Science, Nagoya University.

[‡] Research Center for Materials Science, Nagoya University.

(1) Decher, G.; Hong, J. D.; Schmitt, J. *Thin Solid Films* **1992**, *210/211*, 813−385.

(2) Keller, S. W.; Kim, H. N.; Mallouk, T. E. *J. Am. Chem. Soc.* **1994**, *116*, 8817−8818.

(3) Kotov, N. A.; Dékány, I.; Fendler, J. H. *Adv. Mater.* **1996**, *8*, 637−641.

(4) Kleinfeld, E. R.; Ferguson, G. S. *Science* **1994**, *265*, 370−373.

(5) Kleinfeld, E. R.; Ferguson, G. S. *Chem. Mater.* **1995**, *7*, 2327−2331.

(6) Kotov, N. A.; Dékány, I.; Fendler, J. H. *J. Phys. Chem.* **1995**, *99*, 13065−13069.

(7) Kotov, N. A.; Haraszti, T.; Turi, L.; Zavala, G.; Geer, R. E.; Dékány, I.; Fendler, J. H. *J. Am. Chem. Soc.* **1997**, *199*, 6821−6832.

(8) Kotov, N. A.; Meldrum, F. C.; Fendler, J. H. *Langmuir* **1994**, *10*, 3797−3804.

(9) He, J. X.; Yamashita, S.; Jones, W.; Yamagishi, A.; *Langmuir* **2002**, *18*, 1580−1586.

(10) Park, I. Y.; Kuroda, K.; Kato, C. *J. Chem. Soc., Dalton Trans.* **1990**, 3071.

(11) Carrado, K. A.; Forman, J. E.: Botto, R. E.; Winans, R. E. *Chem. Mater.* **1993**, *5*, 472.

(12) Raki, L.; Rancourt, D. G.; Detellier, C. *Chem. Mater.* **1995**, *7*, 221.

(13) Bonnet, S.; Forano, C.; de Roy, A.; Besse, J. P.; Maillard, P.; Momenteau, M. *Chem. Mater.* **1996**, *8*, 1962.

(14) Takagi, K.; Harata, E.; Shichi, T.; Kanoh, T.; Swaki, Y. *J. Photochem. Photobiol., A* **1997**, *105*, 47.

(15) Gradner, E. A.; Yun, S. K.; Kwon, T.; Pinnavaia, T. J. *Appl. Clay Sci.* **1998**, *13*, 479−494.

(16) Chatti, I.; Ghorbel, A.; Grange, P.; Colin, J. M. *Catal. Today* **2002**, *75*, 113−117.

(17) Allmann, R. *Chimica* **1970**, *24*, 99.

(18) Cavani, F.; Trifiro. F.; Vaccari, A. *Catal. Today* **1991**, *11*, 173.

(19) Hermosin, M. C.; Pavlovic, J.; Ulibarri, M. A.; Cornejo, J. *Water Res.* **1996**, *30*, 171.

(20) Qian, M.; Zeng, H. C. *J. Mater. Chem.* **1997**, *7*, 493.

(21) Xu, Z. P.; Zeng, H. C. *J. Mater. Chem.* **1998**, *8*, 2499.

(22) Ambrogi, V.; Fardella, G.; Grandolini, G.; Perioli, L. *Int. J. Pharm.* **2001**, *220*, 23−32.

(23) Costa, A. S.; Imae, T.; Takagi, K.; Kikuta, K. *Prog. Colloid Polym. Sci.* **2004**, in press.

(24) Costa, A. S.; Imae, T. *Trans. Mater. Res. Soc. Jpn.* **2004**, in press.

10.1021/la049088a CCC: $27.50 © 2004 American Chemical Society
Published on Web 08/24/2004

titative interlayer distance of the intercalated clays and the number of accumulated layers, the morphology of the nanocomposite films was not determined.

Herein, thin films of hydrotalcite and a hydrotalcite/dendrimer nanocomposite at the air/water interface and on a solid substrate were investigated by microscopy techniques. Attention is focused on their morphological characterization. An arachidic acid amphiphilic molecule was used to function as a platform to form clay films. Prior to the film preparation, transmission electron microscopic (TEM) photographs were taken for the estimation of the interlayer distance in the original clay and the nanocomposite. A Brewster angle microscope (BAM) was used to examine the morphology of the films at the air/water interface, and the morphology of the films after transfer onto solid substrates was determined by an atomic force microscope (AFM). Dendrimers are highly branched and topologically regular macromolecules with potential applications in drug delivery,[26] catalysis, and sensors,[27,28] among others. Dendrimer-containing hybrid and layer-by-layer self-assembled films have been explored.[29−39] The monolayer arrangement of dendrimers on a two-dimensional clay platform should result in materials that can be applied as devices, scaffolds, and reaction matrixes.

Experimental Section

Materials. A methanol solution (5 wt %) of generation 4.5 poly(amido amine) dendrimer with sodium carboxylate-terminated groups and chloroform were purchased from Aldrich. Arachidic (eicosanoic) acid (99%) was purchased from Wako Chemical Co. and used as received. Hydrotalcite ($[Mg_{4.5}Al_2(OH)_{13}Cl_2]\cdot 3.5H_2O$) with an anion exchange capacity of 350 mequiv/100 g was donated from Kyowa Chemical Co., Ltd. Mica was furnished by Okenshouji Co. Water purified by a Milli-Q system was used throughout the experiment.

Nanocomposite Preparation. The hydrotalcite/dendrimer nanocomposite was prepared as previously reported.[23] Hydrotalcite was added to the aqueous dendrimer solution to prepare the hydrotalcite/dendrimer mixture at a ratio of 1:4 (anionic charge of clay/carboxyl group of dendrimer). The mixture was incubated for 24 h at 70 °C under shaking. The resulting nanocomposite was filtered using a Millipore filter (0.22-μm pore size), washed with water to remove the excess dendrimer, and dispersed in water at a concentration of 20 mg/cm^3.

Hybrid LB Film Preparation. A 0.4-mm^3 aliquot of arachidic acid solution (0.34 mg/cm^3) in chloroform was spread onto the water subphase (regulated at 25 °C) in addition to a small volume (~1.5 cm^3) of the hydrotalcite/dendrimer nanocomposite suspension (20 mg/cm^3) in a LB film deposition apparatus (Nippon Laser & Electronics). After the chloroform was vaporized for at least 30 min, the surface pressure−area (π−A) isotherms were measured. The film texture, during compression, was investigated by a BAM (Nippon Laser & Electronics) employing a He−Ne laser beam of 632.8 nm.

A Langmuir monolayer of arachidic acid was compressed to the target surface pressure (35 mN/m) at a speed of 10 mm/min and upstroke-transferred to freshly cleaved mica at a transfer speed of 3 mm/min to obtain a Z-type LB film. The nanocomposite-adsorbed arachidic acid Langmuir monolayer was compressed to 35 mN/m at a rate of 10 mm/min and then transferred vertically downward as an X-type film onto the arachidic acid Z-type LB film. Prior to the preparation of the nanocomposite-adsorbed arachidic acid ZX-type LB film, hydrotalcite-adsorbed and basal arachidic acid ZX-type LB films were prepared by the method mentioned above.

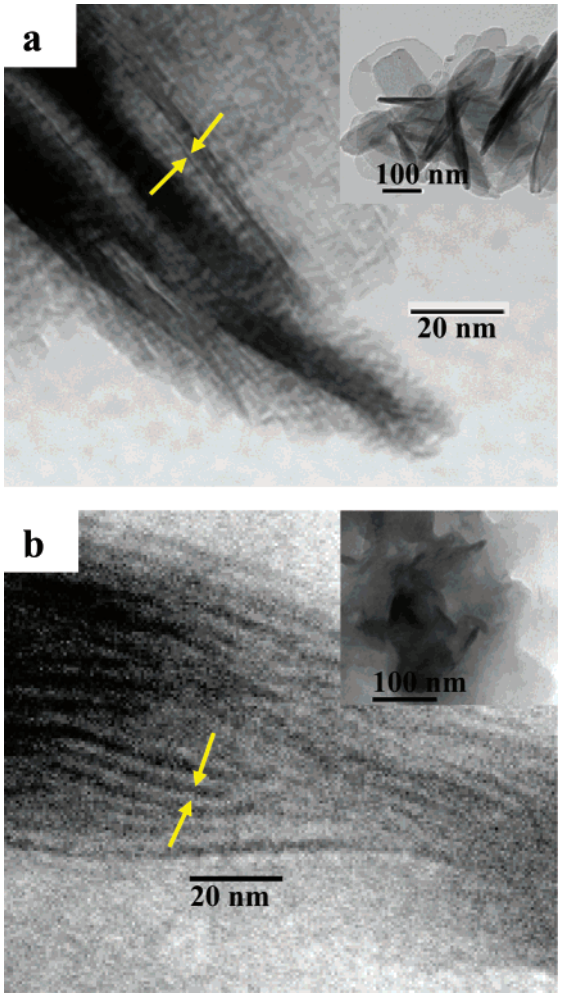

Figure 1. TEM photographs of (a) the original hydrotalcite and (b) the nanocomposite attained after the dendrimer diffusion into the clay interlayers.

Microscopic Observations. TEM photographs were obtained with a Hitachi H-7000 electron microscope, working at an accelerating voltage of 100 kV and equipped with a Hamamatsu C4742-95 digital camera. The specimens were prepared by depositing drops of dispersions of hydrotalcite and nanocomposite onto standard copper grids coated with a carbon film and letting the drops dry completely in the air. AFM measurements were carried out using a Digital Instruments Nanoscope III microscope. The images were taken in contact mode in the air. A silicon tip with spring constant of 0.12 N/m was used.

Results and Discussion

Morphology of the Nanocomposite. The dendrimer diffusion into the interlayers of hydrotalcite through anion exchange results in the intercalation of dendrimer in the

(25) Mitamura, K.; Imae, T. *Trans. Mater. Res. Soc. Jpn.* **2003**, *28*, 71−74.
(26) Esfand, R.; Tomalia, D. A. *Drug Discovery Today* **2001**, *6*, 427−436.
(27) Wells, M.; Crooks, R. M. *J. Am. Chem. Soc.* **1996**, *118*, 3988−3989.
(28) Tokuhisa, H.; Crooks, R. M. *Langmuir* **1997**, *13*, 5608−5612.
(29) Watanabe, S.; Regen, S. L. *J. Am. Chem. Soc.* **1994**, *116*, 8855−8856.
(30) Zhou, Y.; Bruening, M. L.; Bergbreiter, D. E.; Crooks, R. M.; Wells, M. *J. Am. Chem. Soc.* **1996**, *118*, 3773−3774.
(31) Liu, Y.; Bruening, M. L.; Bergbreiter, D. E.; Crooks, R. M. *Angew. Chem., Int. Ed. Engl.* **1997**, *36*, 2114−2116.
(32) Tsuruk, V. V.; Rinderspacher, F.; Bliznyuk, V. N. *Langmuir* **1997**, *13*, 2171−2176.
(33) Tsuruk, V. V. *Adv. Mater.* **1998**, *10*, 253−257.
(34) Zhao, M.; Liu, Y.; Crooks, R. M.; Bergbreiter, D. E. *J. Am. Chem. Soc.* **1999**, *121*, 923−930.
(35) Wang, J.; Chen, J.; Jia, X.; Cao, W.; Li, M. *Chem. Commun.* **2000**, 511−512.
(36) Khopade, A. J.; Caruso, F. *Langmuir* **2002**, *18*, 7669−7676.
(37) Khopade, A. J.; Caruso, F. *Nano Lett.* **2002**, *2*, 415−418.
(38) Alvarez, J.; Sun, L.; Crooks, R. M. *Chem. Mater.* **2002**, *14*, 3995−4001.
(39) Li, C.; Mitamura, K.; Imae, T. *Macromolecules* **2003**, *36*, 9957−9965.

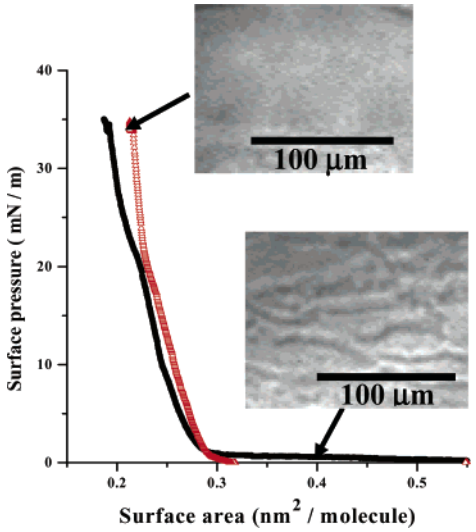

Figure 2. Surface pressure−area isotherms of the arachidic acid monolayer spread onto the aqueous subphase containing hydrotalcite (black curve) and the hydrotalcite/dendrimer nanocomposite (red curve). The insets are the BAM images of the Langmuir films at 0 mN/m (lower inset) and 35 mN/m (upper inset) on subphase containing the hydrotalcite/dendrimer nanocomposite.

clay framework and, hence, the nanocomposite formation. To investigate the morphologies of hydrotalcite and the hydrotalcite/dendrimer nanocomposite, TEM observations were performed. Figure 1 shows their TEM photographs. The neat hydrotalcite presents an irregular size distribution, as Figure 1a (inset) suggests. The layered structure in the particles was confirmed from the dark lines in the TEM images (Figure 1a) as a consequence of the edge-on of the electron beam. The basal hydrotalcite repeating distance around 1.2 ± 0.3 nm can be drawn out from TEM images. The morphology of the nanocomposites was different from the neat hydrotalcite: the nanocomposites showed larger and denser plates [Figure 1b (inset)] due to the dendrimer intercalation, which induces the stacking of hydrotalcite particles, and the basal repeating distance increases to 3.2 ± 0.5 nm (Figure 1b). These morphological structures are consistent with the structures obtained by X-ray diffraction, small-angle X-ray scattering, and X-ray reflection techniques, which were reported previously.[23,25] The X-ray diffraction and small-angle X-ray scattering results indicated the expansion of the basal clay distance from 0.8 nm in the neat clay to 2.5−2.8 nm in the nanocomposites.[23] The values of 1.0 and 3.3 nm for neat clay and nanocomposites, respectively, were evaluated from X-ray reflection analysis.[25]

Characterization of Hybrid Langmuir Films at the Air/Water Interface. The $\pi-A$ isotherms of the arachidic acid Langmuir monolayer on hydrotalcite and hydrotalcite/dendrimer nanocomposite subphases are presented in Figure 2. Under the continuous compression, the surface pressure in the gas phase started increasing at a surface area of 0.29 nm^2/molecule on both hydrotalcite and nanocomposite subphases. Through the transition from the liquid-expanded to the liquid-condensed phase, the solid monolayer phase was formed above 25 and 20 mN/m on the hydrotalcite and nanocomposite subphases, respectively. The further compression on both subphases resulted in a steep rise in the surface pressure up to 35 mN/m, which is a collapsed pressure. The occupied surface areas, which were evaluated from the extrapolation of the straight line at the solid phase in the $\pi-A$ curve down to the surface area axis, were 0.237 and 0.243 nm^2/molecule

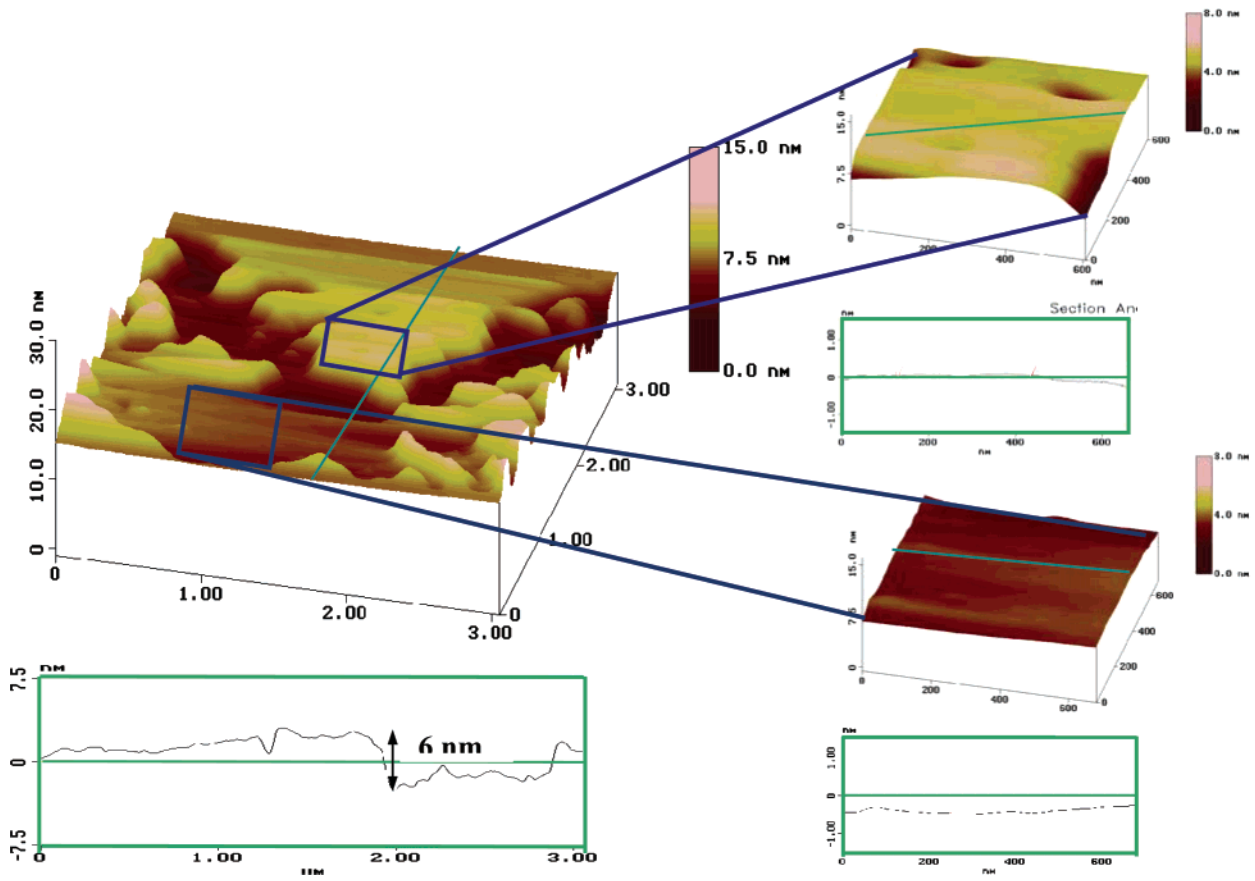

Figure 3. AFM image of the arachidic acid ZX-type LB film containing bound hydrotalcite. The figure displays expanded regions of the arachidic acid and hydrotalcite surfaces and the accompanying cross-sectional profiles.

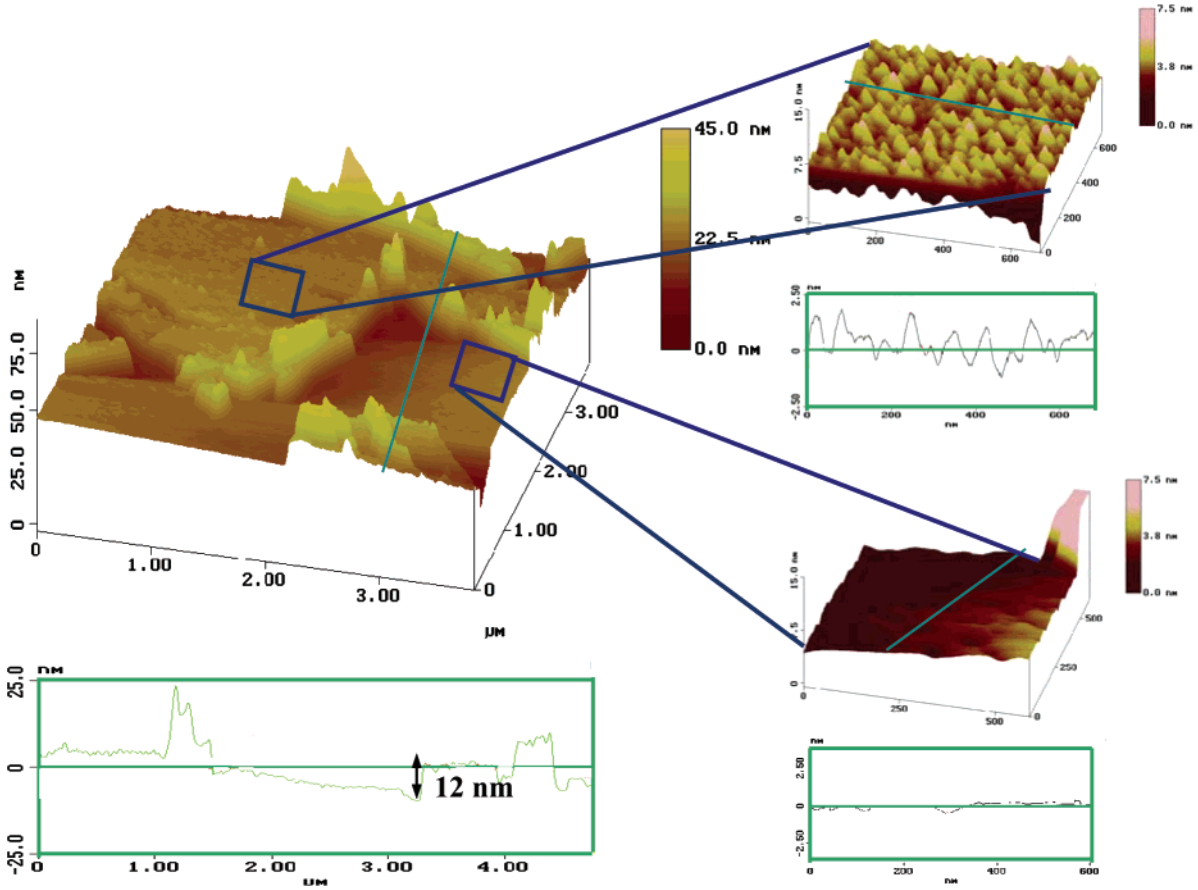

Figure 4. AFM image of the arachidic acid ZX-type LB film containing the bound hydrotalcite/dendrimer nanocomposite. The figure displays expanded regions of the arachidic acid and hydrotalcite/dendrimer nanocomposite surfaces and the accompanying cross-sectional profiles.

on the hydrotalcite and nanocomposite subphases, respectively. Despite the close values of the occupied surface area on hydrotalcite and nanocomposite subphases, these values are slightly larger than that for the arachidic acid monolayer (0.195 nm^2/molecule) previously reported.[40] This difference is due to the adsorption of hydrotalcite and nanocomposite onto the arachidic acid monolayer.

The recording of the $\pi-A$ isotherm was simultaneously accompanied by BAM to monitor the morphological changes in the Langmuir monolayer on the subphase. BAM images taken on the arachidic acid monolayer revealed a gradual increase in the density number of floating domains upon compression (data not shown). The circular oil-like domains gradually packed up to form a uniform monolayer at a surface pressure of 35 mN/m. BAM images on both hydrotalcite and nanocomposite subphases at zero surface pressure also showed the presence of (platelike) domains with irregular sizes that conglomerated to turn into a uniform layer, as shown in Figure 2. The similar profiles for both hydrotalcite and the nanocomposite indicate the independence of the intercalation of dendrimer on the adsorption of clay onto arachidic acid monolayer.

Morphology of Hybrid LB Films on the Substrate. AFM images of arachidic acid ZX-type LB films of adsorbed hydrotalcite were taken, and the surface coverage and homogeneity of the hydrotalcite film were compared at varying conditions, regarding the incubation times at zero surface pressure after the spread of the solution and at 35 mN/m after the compression. The AFM image obtained for the films prepared at longer incubation times at zero surface pressure showed the presence of many clay domains on the arachidic acid surface. The clay particles were accumulated with a height difference of maximum 45 and 95 nm at 30 and 120 min of incubation, respectively, forming an inhomogeneous film. On the other hand, the 120 min of incubation at 35 mN/m brought about homogeneous coverage by clay particles on the arachidic acid surface. The height difference was about 6−8 nm, independent of the incubation time at zero surface pressure. The preparation condition, in which the immediate compression after spreading of arachidic acid on the subphase is followed by a 120 min incubation at 35 mN/m, was used throughout the experiments hereafter.

An AFM image of hybrid ZX-type LB film of arachidic acid and hydrotalcite is shown in Figure 3. The image indicated the presence of platelike clay stacks with a good extent of coverage on the arachidic acid surface. The surface analysis revealed the smoothness of both the clay platelets and the arachidic acid LB film. The latter surface is similar to that of the basal arachidic acid ZX-type LB film (figure is not shown). The AFM image of the hybrid LB film with the nanocomposite (Figure 4) pointed out the stack of clay layers with a thickness of about 12 nm. The surface analysis of the clay top showed the presence of many small islands ranging around 2 nm in height and 35−45 nm in width, similar to that of the dendrimer thin film.[41]

Interactions among Dendrimer, Hydrotalcite, and Arachidic Acid. The TEM and AFM observations sug-

(40) Mori, O.; Imae, T. *Langmuir* **1995**, *11*, 4779−4784.

(41) Imae, T.; Funayama, K.; Aoi, K.; Tsutsumiuchi, K.; Okada, M.; Furusaka, M. *Langmuir* **1999**, *15*, 4076−4084.

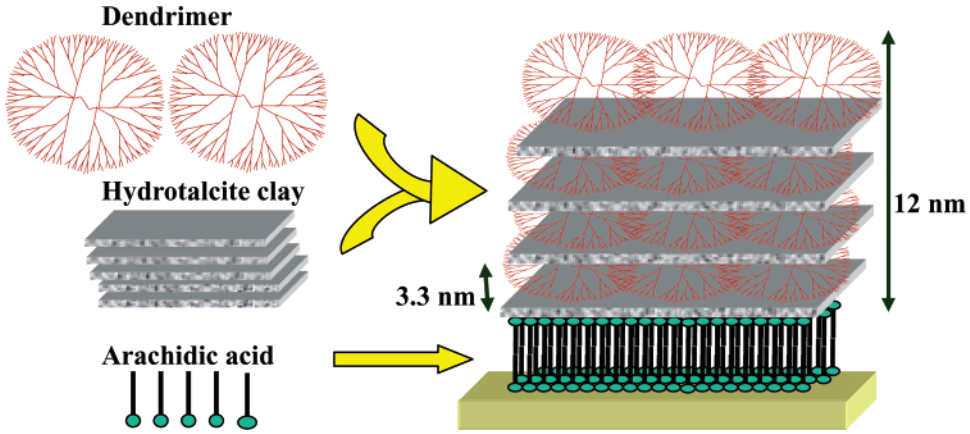

Figure 5. Schematic illustration of the arachidic acid ZX-type LB film containing the bound hydrotalcite/dendrimer nanocomposite.

gested the presence of dendrimers intercalated into and adsorbed onto hydrotalcite. The repeating distance (3.2 ± 0.5 nm) found in the nanocomposite is correlated well to a model, where the dendrimer molecules are sandwiched between clay layers in a shape distorted from the spheroid in solution.[23] Then the interaction between clay and dendrimer is the electrostatic attraction between negative charges of carboxyl groups in dendrimer and positive charges developed in the hydrotalcite clay structure.

Domains in the hybrid Langmuir monolayer of arachidic acid and the nanocomposite were irregular in size and shape at the initial surface pressure. At higher surface pressures, the hybrid domains conglomerated to form the uniform film, as observed in a BAM photograph. The hybrid monolayer was more homogeneous and stable (no collapse) when maintained at a pressure of 35mN/m for 2 h. This arises from the self-organization of nanocomposites on the arachidic acid monolayers. The accumulation of clay may occur from the interclay interaction by the intervention of dendrimers on the clay surface, where the electrostatic interaction sways.

The incubation of hybrid monolayer for 2 h at a surface pressure of 35 mN/m resulted in the uniform film. This indicates the strong interaction between the arachidic acid monolayer and the nanocomposite as well as the interaction between nanocomposites.The hydrogen bonding between the carboxyl groups of arachidic acid and carboxyl groups of the dendrimer on hydrotalcite might be the main factor in the adhesion of hydrotalcite nanocomposite to the arachidic acid monolayer. X-ray reflectometric results[25] suggested that the arachidic acid molecules are directly connected to the clay surface, indicating that there is no dendrimer on the clay surface faced to the arachidic acid ZX-type LB film. Thus, it should be supported that the interaction arises from the electrostatic attraction between the negatively charged carboxyl group of the fatty acid and the positive charge in the brucite-like outermost clay layer. This is possible in the alkaline solutions that were examined in the present work. This is an indication that the hydrotalcite/arachidic acid interaction is stronger than the hydrotalcite/dendrimer interaction. Figure 5 illustrates the plausible model of the hybrid LB film.

Conclusions

The morphology of hydrotalcite and the hydrotalcite/dendrimer nanocomposite obtained by the ionic exchange process was investigated. The increase of the basal distance of the hydrotalcite upon the dendrimer intercalation was evidenced from TEM pictures. The subsequent preparation and characterization of hydrotalcite and the nanocomposite film on the arachidic acid monolayer used as a template were performed, and BAM pictures evidenced the packing up of nanocomposite particles, which resulted in a compact film. The monolayers were transferred as uniform LB films onto mica, as observed in the AFM pictures. The heights and morphology of hydrotalcite and nanocomposite stacks on the arachidic acid film proved the dendrimer intercalation and the presence of dendrimers on the top of clay stacks. The obtained hybrid film may be useful as scaffolds for subsequent organizations.

Acknowledgment. A.S.C. acknowledges the Ministry of Education, Culture, Sports, Science and Technology, Japan, for the award of a graduate scholarship (Monbukagakusho scholarship).

LA049088A